An Accurate Acetylene Intermolecular Potential for Phase Behavior Predictions from Quantum Chemistry

Stephen L. Garrison and Stanley I. Sandler*

Department of Chemical Engineering, Center for Molecular and Engineering Thermodynamics, University of Delaware, Newark, Delaware, 19716

Received: March 22, 2004; In Final Form: June 14, 2004

We have developed an ab initio potential for acetylene by computing interaction energies for a range of orientations and center-of-mass separation distances. These energies are initially fit with a simple weighting scheme to a pairwise-additive, site−site Morse-C_6 intermolecular potential. Additional interaction energies were then calculated at separation distances determined to be important from the center-of-mass radial distribution function calculated from molecular simulation with use of the initial potential. The expanded set of interaction energies is then fit using Boltzmann-like weighting to obtain an improved intermolecular potential. The phase behavior calculated from Gibbs ensemble Monte Carlo simulations using this improved potential is in excellent agreement with experimental data. Also, the results of *NVT* ensemble Monte Carlo calculations show good agreement with experimental data at supercritical temperatures and pressures, and results are presented for conditions that would be hazardous experimentally. Additionally, the second virial coefficients calculated using this potential indicate that one set of experimental data reported in the literature is likely to be erroneous. The prescription described here for obtaining the optimum potential from quantum chemical methods should be applicable to other systems.

Introduction

With the rapid increase in available computational resources, molecular simulations are now frequently used to calculate a wide range of thermodynamic properties of interest to scientists and engineers. Molecular simulations can be used to provide an understanding of fundamental molecular processes, especially when the time scales, length scales, or conditions are not easily amenable to experiment. However, reliable prediction, and not just correlation, of thermodynamic properties using molecular simulations requires accurate intermolecular potentials. Such potentials can, in principle, be obtained from quantum chemistry thus allowing researchers to predict macroscopic properties without resorting to an empirically fit potential that may have a limited range of validity. Furthermore, results calculated from ab initio potentials can also help resolve discrepancies in experimental data, as we show here.

Calculation of the intermolecular interaction energies necessary to develop accurate potentials for many systems, especially weakly interacting systems, generally requires computationally intensive quantum chemical methods such as CCSD(T) or QCISD(T). Also, large basis sets are required to adequately describe the wave function in these calculations. For molecular systems of reasonable size, this combination of high-level quantum chemical methods and large basis sets is prohibitively expensive computationally. However, a recently introduced hybrid extrapolation method, the Hybrid Method for Interaction Energies (HM-IE),[1] provides a technique to approximate the results from high-level quantum chemical methods and large basis sets in a computationally efficient manner so that accurate interaction energies for larger systems can be obtained in a reasonable amount of time.

Even with precise quantum chemical interaction energies, there remains the problem of developing an accurate and analytic intermolecular potential. Uncertainties arise from the choice of analytical expression for the potential, the fitting and weighting procedures used, and the configurations at which interaction energies were computed. (We define a configuration as the combination of the relative molecular orientation and the center-of-mass (COM) separation distance.) Previous work on how the calculated phase behavior of an atomic system is affected by perturbations to an interaction potential[2] provides some guidance concerning the choice of configurations and weighting procedures for molecular systems.

Acetylene is one example of a relatively simple molecular system that can be difficult experimentally. A mixture of acetylene and air has a wider range of concentrations where it is flammable and a lower autoignition temperature at atmospheric pressure than a mixture of hydrogen and air, 2.5% to 80% compared to 4% to 75% and 578 K versus 773 K, respectively. As a result of this reactivity and instability, an apparatus failure during the collection of *PVT* data in high-temperature experiments could result in a catastrophic explosion. Hence, acetylene is an excellent example of a system where the calculation of thermodynamic properties using molecular simulation, instead of determination by experiment, would be advantageous.

This work focuses on choosing appropriate intermolecular configurations at which accurate interaction energies are calculated by using the Hybrid Method for Interaction Energies and then fitting these energies to obtain a pairwise-additive, intermolecular potential for use in molecular simulations of acetylene. Using Gibbs ensemble Monte Carlo simulations and the intermolecular potential obtained, the vapor−liquid-phase behavior of acetylene is computed and found to be in excellent agreement with experimental data even though no experimental

* To whom correspondence should be addressed. E-mail: sandler@udel.edu. Phone: (302) 831-2945. Fax: (302) 831-3226.

10.1021/jp048731z CCC: $27.50
Published on Web 11/13/2004

data were used to obtain this potential. Also, high-temperature *PVT* behavior calculated from *NVT* ensemble Monte Carlo simulations is in good agreement with available experimental data, and additional calculations are made at conditions that would be hazardous experimentally. Finally, the second virial coefficients computed from this new potential are used to resolve a discrepancy in the reported experimental data.

Methods

For weak interactions such as those between acetylene molecules, researchers[3−8] have found that the use of bond functions (bf) [a small set of basis functions located between two molecules] can significantly improve the description of the wave function, especially in the region between the two molecules. This improvement results in more accurately calculated interaction energies with only a small increase in computational cost, and is especially useful in high-level, quantum chemical calculations, such as CCSD(T) calculations. In this work, we have used a 3s2p1d set of basis functions as bond functions with exponents similar to those in previous work.[1,5] (The exponents used are 0.553, 0.251, and 0.117 for the s shells; 0.392 and 0.142 for the p shells; and 0.328 for the d shell.) For all calculations, we placed the bond functions between the two molecules at the COM of the system.

Even with bond functions, CCSD(T) calculations are computationally expensive. Recently, a new method for the calculation of interaction energies, HM-IE, was introduced[1] to accurately approximate CCSD(T) energies with a large basis set (LBS) for a wide range of systems but with a significant reduction in computational cost. Briefly, the interaction energy from HM-IE is obtained in a manner similar to the Gaussian-3 (G3) method[9,10] or the methods of Dunning and Peterson.[11] As MP*n* calculations (where *n* is generic for 2 or 3) are significantly less computationally intense than CCSD(T) calculations, the difference in energy at the CCSD(T) level between using a LBS and a small basis set (SBS) is approximated by the difference in energy between the two basis sets at the MP*n* level. That is, using the notation that *E*[...] is a calculated interaction energy, the HM-IE energy *E*[MP*n*:CC] is defined as follows:

$$E[\mathrm{MP}n\mathrm{:CC}] \equiv E[\mathrm{CCSD(T)/SBS}] + (E[\mathrm{MP}n\mathrm{/LBS}] - E[\mathrm{MP}n\mathrm{/SBS}]) \quad (1)$$

Averaging the energies from HM-IE at the MP2 and MP3 levels, *E*[MP2/3:CC], was found to give the most accurate results overall[1] and is the method used here to calculate interaction energies. All calculations were performed with Gaussian98,[12] and the counterpoise correction method[13] was used to remove[14] the basis set superposition error[15] that occurs in supermolecular calculations such as those performed here. As previous researchers have found that molecular flexibility has little effect on simulation results for nonpolar molecules,[16,17] the bond lengths were fixed for all calculations at the equilibrium bond lengths, $R_{CH} = 1.062$ Å and $R_{CC} = 1.204$ Å.[18]

To determine the most appropriate basis set to use, we compared interaction energies computed at the CCSD(T) level for three orientations at the COM separation distances where each orientation is a symmetry constrained minima: (1) the "T-shaped," minimum energy orientation with C_{2v} symmetry; (2) the "slipped parallel" orientation that is a first-order saddle point with C_{2h} symmetry with a 42° angle between the axis of one molecule and a line connecting the COM of each molecule; and (3) the "cross-shaped" orientation that is a second-order saddle point with D_{2d} symmetry in which the two molecules

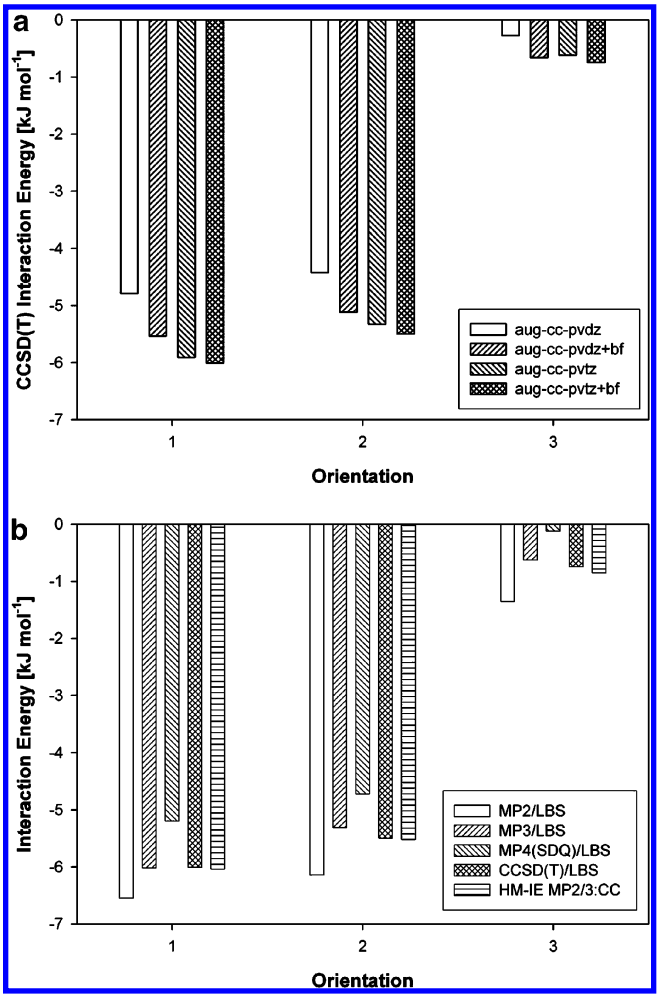

Figure 1. Interaction energies for three symmetry constrained minima of acetylene: (a) CCSD(T) interaction energies as a function of basis set and (b) interaction energies as a function of theory level. LBS is aug-cc-pvtz+bf and SBS is 6-31+g(d,p)+bf. Orientations: (1) "T-shaped" orientation with C_{2v} symmetry; (2) "slipped parallel" orientation with C_{2h} symmetry; and (3) "cross" orientation with D_{2d} symmetry.

are perpendicular to each other but out of plane.[19] For acetylene, the 16GB limitation of accessible and addressable scratch disk space when using Gaussian98 on 32-bit machines prevents the use of Dunning's correlation-consistent basis sets larger than aug-cc-pvtz either with or without bond functions. However, as seen in Figure 1a, the CCSD(T) energy of each configuration as a function of increasing basis set size is nearing a plateau with the aug-cc-pvtz+bf basis set. For these reasons, we chose to use the aug-cc-pvtz+bf basis set as the LBS. For the SBS, we used the 6-31+g(d,p)+bf basis set.

Figure 1b shows that, for all three configurations, there are noticeable differences between the energies calculated at various levels of theory with use of the aug-cc-pvtz+bf basis set. In particular, the MP2 and MP4(SDQ) results differ significantly from the more accurate CCSD(T) results, while the MP3 results deviate considerably less. (In the more thorough analysis of the various methods in previous work,[1] MP3/LBS was found to be the most accurate of the non-HM-IE methods, but its average and maximum deviations were larger than those obtained with MP2:CC, MP3:CC, and MP2/3:CC.) We see that the results of the HM-IE MP2/3:CC calculation, with the 6-31+g(d,p)+bf basis set as the SBS, give energies that differ from the CCSD(T)/LBS results by only between 0.01 and 0.1 kJ/mol. This small difference is acceptable, especially given that the

TABLE 1: Parameter Values for the HM-IE MP2/3:CC Potentials

(a) Initial Potential

site−site pair	ϵ [kJ mol^{-1}]	α [Å^{-1}]	r_m [Å]	C_6 [Å^6 kJ mol^{-1}]	d_1 [Å^{-1}]	d_6 [Å^{-1}]
H−H	2.67784×10^{-7}	1.92166	6.16426	106.670	9.94674	0.758667
H−C	9.10776×10^{-2}	1.46968	3.83981	1255.47	8.01124	2.46794
H−COM	6.28020	12.4915	2.03728			
C−C	2.64164×10^{-5}	1.34652	7.58474	1000.99	1.76052	1.76053
C−COM	1.20042×10^{-13}	7.41900	5.04687			

(b) Final Potential

site−site pair	ϵ [kJ mol^{-1}]	α [Å^{-1}]	r_m [Å]	C_6 [Å^6 kJ mol^{-1}]	d_1 [Å^{-1}]	d_6 [Å^{-1}]
H−H	3.49818×10^{-6}	0.468660	15.6587	106.670	6.70726	0.607250
H−C	1.00699	1.61878	2.99965	1255.47	2.06778	2.06751
H−COM	3.47675	7.15524	2.24017			
C−C	1.06816×10^{-9}	0.929798	15.5002	1000.99	1.44603	0.620288
C−COM	3.48337	1.91559	3.20750			

computational time for one configuration is reduced from 41 h for a CCSD(T)/LBS calculation to 7.5 h for a HM-IE MP2/3:CC calculation. (All calculations were performed with an AMD MP1800+ processor.)

The most common (and therefore most important) relative molecular orientations of acetylene molecules in the liquid phase are not known a priori. In an attempt to adequately cover the entire range of possible molecular orientations, we chose to use the quasirandom low-discrepancy sequence implemented in the IMSL C Math Library to generate orientations for which to calculate interaction energies. In comparison to traditional pseudorandom number generators, a low-discrepancy sequence covers space more uniformly, and adding more orientations from a low-discrepancy sequence to improve the coverage is simpler than refining a grid.

In addition to orientation, we do not know a priori the most probable or most important COM separation distances in the liquid phase. However, we do know that the COM separation distance of the minimum energy configuration for a pair of molecules, r_{min}, is 4.4 Å. Therefore, we calculated interaction energies for 20 initial orientations at COM separation distances of 3.4, 3.9, 4.4, 4.9, and 5.4 Å, or from approximately $0.75r_{min}$ to $1.25r_{min}$. Interaction energies were also calculated for the minimum energy orientation for the same five separation distances resulting in a total of 105 different configurations.

To obtain an initial estimate of the potential, these interaction energies were fit to a pairwise-additive, site−site potential function combining a Morse potential, a damped C_6 dispersion term, and a damped charge−charge term

$$U = \sum_{a\in A}\sum_{b\in B}\left[\epsilon_{ab}([1 - \exp(\alpha_{ab}[r_{m,ab} - r_{ab}])]^2 - 1) - f_6(d_{6,ab}\, r_{ab})\frac{C_6}{r_{ab}^{\,6}} + f_1(d_{1,ab}\, r_{ab})\kappa\frac{q_a q_b}{r_{ab}}\right] \quad (2)$$

where U is the energy between two molecules; a and b are sites on molecules A and B; ϵ is the well depth, α is the "steepness", and r_m is the location of the minimum of the Morse term; d_1 and d_6 are damping parameters; q is the charge of a site and κ is the Coulomb constant; r is the distance between sites a and b; and f is the Tang−Toonies damping function, eq 3.

$$f_n(x) = 1 - e^{-x}\left(1 + \sum_{i=1}^{n}\frac{x^i}{i!}\right) \quad (3)$$

Equation 2 was chosen because it includes terms to represent dispersion, long-range electrostatics, and short-range interactions that reasonably describe the molecular interactions without being too computationally expensive or having too many parameters.

TABLE 2: Saturation Properties of Acetylene from GEMC Simulations, Using the Final HM-IE MP2/3:CC Potential

temp [K]	liquid density [g/cm^3]	vapor density [g/cm^3]	vapor pressure [bar]
200	0.6203	0.0036	2.26
225	0.5796	0.0098	6.31
235	0.5622	0.0140	9.08
250	0.5316	0.0235	15.1
265	0.4994	0.0395	23.7
275	0.4701	0.0516	31.1
290	0.4170	0.0838	45.3
303.6[a]	0.241	0.241	61.5

[a] Estimated critical point.

Initially, interaction sites were placed only on each atom, but significant improvement in the fit was obtained by adding an additional site at the COM of each molecule. (While the site at the COM was added empirically to improve the fit, it may have physical significance due to the π electrons of the triple bond between the carbon atoms). The limited number of COM-COM separation distances (compared to all other site-site pairs) resulted in numerical instabilities during the fitting of the potential. Therefore, the COM-COM site-site potential was set to zero. Charges were only placed on the atomic sites and were chosen to duplicate the average of the reported experimental quadrupole moments, 6.17 D Å. The charges used were 0.267 e on each hydrogen atom and −0.267 e on each carbon atom. The energy of each configuration was weighted equally (ignoring configurations with highly repulsive energies greater than +40 kJ/mol), and the fitting algorithm alternated between the nonlinear least-squares routine in the IMSL C Math Library and a simplex routine until an overall convergence was achieved. Additionally, the dispersion terms were fit separately to long-range, asymptotic energies calculated from the electrical moments of a single molecule with the POLCOR programs[20,21] and then fixed for the remainder of the fit. The damping parameters were fit using the energies at the largest COM separation distance and then fixed for the remainder of the fit to control the behavior of the potential at long range.

The parameters obtained for the five site−site interaction pairs are found in Table 1a. The small values of ϵ for several of the interaction pairs indicate that those site−site potentials could be well represented by a two-parameter exponential repulsion model without an attractive region instead of the three-parameter Morse model used here. Specifically, the hydrogen−hydrogen potential (H−H) is repulsive except at very large separation

TABLE 3: Thermodynamic Properties of Supercritical Acetylene

	pressure [bar]		
density [g/cm^3]	323.15 K	523.15 K	723.15 K
0.001	1.03	1.67	
0.005	5.04	8.30	
0.010	9.88	16.6	23.2
0.025	23.0	40.8	
0.050	41.4	80.4	117
0.100	66.1	157	241
0.150	80.3	233	
0.200	87.2	319	538
0.250	95.6	424	
0.300	97.1	553	971
0.350	118		
0.365	128		
0.385	138		
0.400	163		1700

distances when charge−charge interactions are neglected and repulsive at all separation distances when charge−charge interactions are included. This is consistent with previous work,[22,23] and is not merely the result of the addition of the COM interaction site as similar behavior was found when the potential was restricted to only atom−atom interactions. Significant departure from the empirical Lorentz−Berthelot mixing rules for the well-depth and distance parameters ϵ and r_m, respectively, was found for the interaction parameters between unlike sites, e.g. the hydrogen−carbon interaction. One advantage of obtaining interaction potentials from quantum chemistry is that, by fitting parameters for all site−site interaction pairs, both like and unlike, we are not constrained to use the Lorentz−Berthelot mixing rules that have been shown to be inadequate.[24]

The potential was then used in *NVT* Gibbs ensemble Monte Carlo (GEMC) simulations in which the total number of molecules N (512), the total system volume V, and the temperature T were held constant. Simulations were run at five temperatures, 225, 250, 265, 275, and 290 K. Approximately 20 000 cycles were used for equilibration and each production run lasted at least 40 000 cycles in which one cycle consisted approximately of 512 translations, 512 rotations, one volume exchange, and a sufficient number of particle exchanges to average slightly more than one exchange per cycle. To ensure microscopic reversibility, each molecule and move were chosen randomly, as was the box from which the molecule was chosen, and standard long-range corrections to the pressure and energy[25] were applied. Using the densities at the four highest temperatures, the critical temperature T_c and the critical density ρ_c were fit by using renormalization group theory (eq 4) and the law of rectilinear diameters (eq 5).[26]

$$\rho_l - \rho_v = A(T_c - T)^\beta \tag{4}$$

$$\frac{\rho_l + \rho_v}{2} = \rho_c + B(T_c - T) \tag{5}$$

The critical exponent β was included as a fit parameter and ranged from 0.287 to 0.308. The critical pressure was estimated by fitting the vapor pressures P^{vap} from simulation to eq 6 and then solving for P^{vap} at T_c.

$$\ln[P^{vap}] = C_1 + \frac{C_2}{T} \tag{6}$$

Results and Discussion

Figure 2 shows the vapor−liquid-phase behavior obtained from the GEMC simulations using the initial potential, indicated by the squares. While the densities at the lower temperatures are in reasonable agreement with experiment,[27−30] there are significant errors at higher temperatures, and the vapor pressures are too low at all temperatures. Even though there are differences between the experimental data and the simulation results, we expect that the most common orientations and separation distances in the dense phase obtained from the COM radial distribution function and the angular distribution for these simulations would likely also be important in simulations with an improved potential. This information, therefore, was used to identify additional important orientations and COM separation distances at which interaction energies should be calculated.

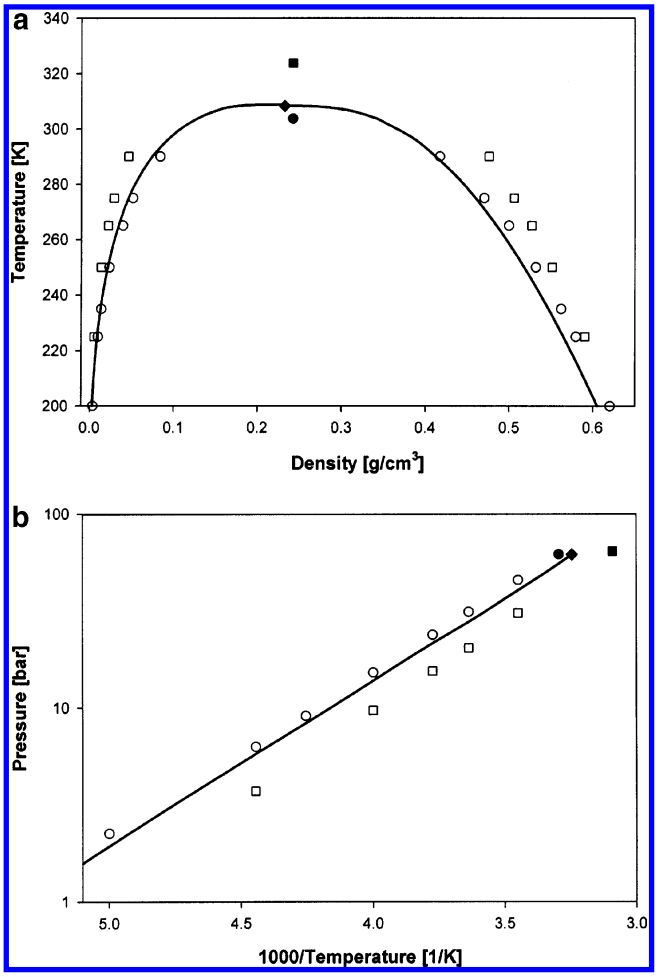

Figure 2. Vapor−liquid-phase behavior for acetylene: (a) saturated density curve and (b) vapor pressures. The line is the experimental results,[27−30] the squares are the results with the initial HM-IE MP2/3:CC potential, and the circles are the results with the final HM-IE MP2/3:CC potential. Filled symbols are the (estimated) critical points.

In previous work on atomic systems,[2] it was found that small changes to the repulsive region affected the calculated phase behavior very little, whereas small changes in the long-range region, the well region, and the crossing point (the separation distance at which the potential is zero) significantly altered the calculated vapor−liquid-phase behavior. Therefore, we examined the liquid-phase COM pair distribution function to determine regions where additional interaction energies should be calculated. (We chose to investigate the results at the middle temperature of 250 K to balance the effects of higher temperatures with those of higher density.)

For an atomic system in the low-density limit, the radial distribution function is a maximum at the separation distance at which the potential is a minimum, i.e., the potential well,

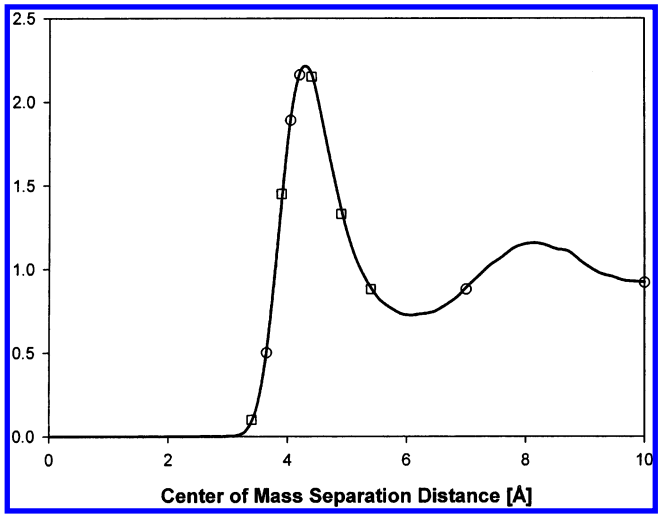

Figure 3. Center-of-mass pair distribution function for the saturated liquid phase from simulation at 250 K using the initial HM-IE MP2/3:CC potential. (The density is 0.55 g/cm^3.) The squares are the center-of-mass separation distances included in the initial potential. The circles are the additional separation distances added for the final potential. The *y*-values for the squares and circles were chosen to indicate approximate location on the center-of-mass pair distribution function.

and is unity at the separation distance at which the potential is zero, i.e., the crossing point. For the discussion of a molecular system that follows, we chose to define the well region as the COM separation distances at or near the first maximum in the COM radial distribution function and to define the crossing point as the COM separation distance at which the liquid-phase COM radial distribution function is unity before the first maximum.

We see in Figure 3 that, of the interaction energies calculated initially, only one COM separation distance falls within the well region. Therefore, to improve the description of the well region, we calculated interaction energies for the original 20 orientations at additional COM separation distances of 4.05 and 4.2 Å. To improve the description of the crossing point, we calculated energies for these same orientations at an additional COM separation distance of 3.65 Å, halfway between the two COM separation distances closest to the crossing point. To ensure that the new potential would adequately represent the long-range region, we also calculated interaction energies at additional COM separation distances of 7.0 and 10.0 Å, or about 1.6 and 2.3 r_{min}. We also calculated energies at all ten COM separation distances for an additional 30 quasirandom orientations, resulting in a total of 505 configurations.

Previously, it has been suggested that the minimum energy configuration is important for determining an accurate intermolecular potential.[31] To help accurately represent the potential around this orientation in that work, interaction energies were calculated for a significant number of additional configurations that were slight perturbations in orientation or COM separation distance from the minimum energy configuration. From a simulation snapshot of molecule locations at 250 K using the initial potential, we calculated how frequently two molecules in the liquid phase were found with a particular angle ϕ (defined in Figure 4) between the axis of one molecule and a line connecting the COM of the two molecules (ignoring the remaining two angles needed to fully specify the orientation).

As indicated by the filled circles in Figure 5a, the frequency of finding two molecules in the T-shaped or similar orientation, where ϕ is near 0°, is almost zero even though the Boltzmann factors of the interaction energies for these orientations would suggest that they should occur more often in simulation. This

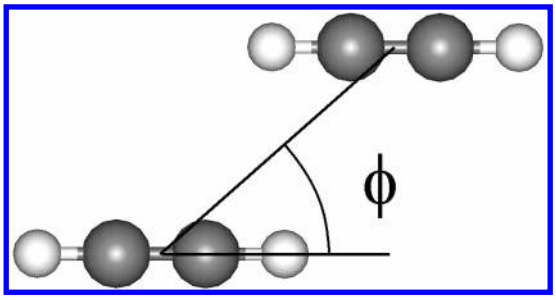

Figure 4. Diagram of the angle ϕ between two acetylene molecules.

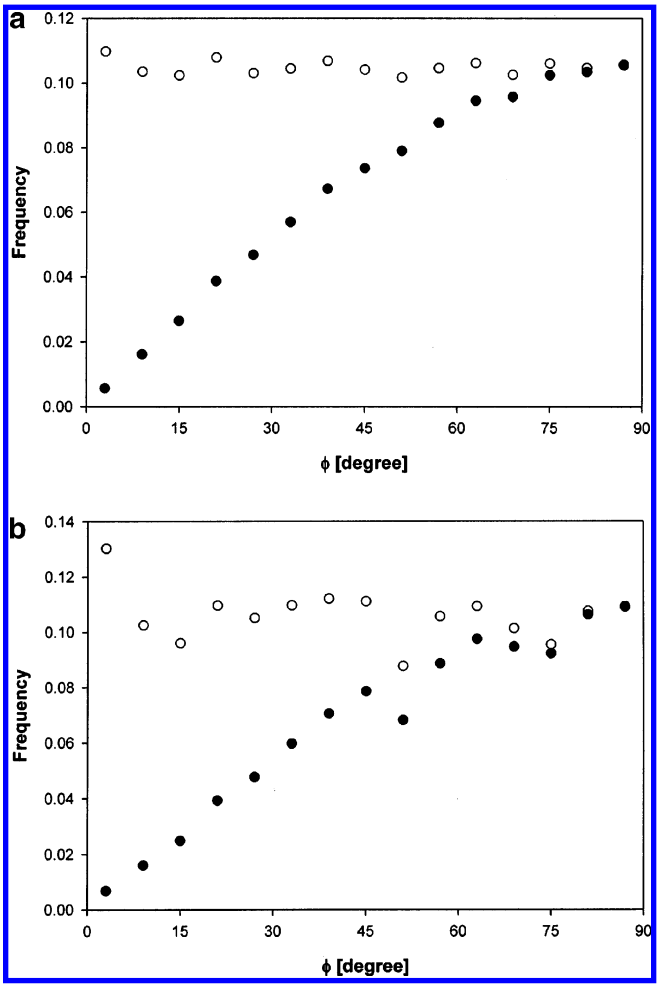

Figure 5. Frequency of finding two molecules in the liquid phase at 250 K with an angle ϕ between the axis of one molecule and the line connecting the two molecular centers of mass: (a) all molecular pairs and (b) all molecular pairs with center-of-mass separation distances less than 6 Å. The filled circles are the frequencies. The open circles are the frequencies normalized by sin ϕ.

difference arises because the total frequency also depends on the surface area swept out by rotating the first molecule around the line connecting the COM of the two molecules, that is, the total frequency is proportional to sin ϕ. The open circles in Figure 5a illustrate that, when normalized by sin ϕ, the T-shaped orientation and similar orientations with small values of ϕ are slightly more likely to occur than other orientations.

Looking only at molecules with COM separation distances of 6 Å or less (separation distances up to approximately the first minimum in the distribution function, i.e., the first coordination shell), we see a change in the distribution of orientations. The T-shaped orientation again does not occur frequently except when normalized by sin ϕ. There are slight

preferences for orientations with an angle of about 20° and against orientations with angles of about 50° and 75°; however, there is scatter in the data due to the limited number of molecular pairs within the first coordination shell.

Knowing that the T-shaped and similar orientations occur infrequently, it is unlikely that these orientations are important in the description of the liquid phase. This indicates that the previously reported importance of the minimum energy configuration may have been overemphasized except for cases where the minimum energy configuration occurs frequently within simulation, and no calculations were performed for additional configurations near the minimum energy configuration.

Analysis of the pair interaction energies also indicates that the range of energies found during simulation is quite limited. In the same simulation snapshot as earlier, less than one percent of the configurations with COM separation distances of 6 Å or less have pair interaction energies greater than +2 kJ/mol. Given that the number of configurations with interactions energies greater than +2 kJ/mol is miniscule, the contribution of these configurations to the thermodynamic properties should be minimal, and therefore, they were not included in the final fit. A new potential was then obtained by refitting the potential to the combination of the initial and newly calculated quantum chemical interaction energies. To better represent the important attractive energies during the fitting, we used a Boltzmann-like weighting function

$$w_i = 1 + e^{[(E_i - E_{min})/E_{min}]} \quad (7)$$

where w_i is the weight for configuration i, E_i is the energy of configuration i, and E_{min} is the energy of the minimum energy configuration (about −6 kJ/mol). The new potential parameters obtained in this way are reported in Table 1b, and we refer to this potential as the final potential.

The initial potential fit the initial set of configurations with energies less than +40 kJ/mol relatively well (0.26 kJ/mol RMSD), but failed to accurately predict the vapor−liquid-phase behavior. When this potential was then compared with the additional orientations and COM separation distances we subsequently calculated (but only for configurations with energies less than +2 kJ/mol), the RMSD for the initial potential was again rather good (0.013 kJ/mol (RMSD). However, by focusing on accurately fitting the attractive orientations in the well, long-range, and crossing-point regions that are likely to occur in simulation, the final potential more accurately describes these important regions of the potential energy landscape and has a RMSD of only 0.005 kJ/mol for configurations with energies less than +2 kJ/mol.

By using the final potential in GEMC simulations, much better agreement with the experimental phase behavior is obtained as indicated by the circles in Figure 2. The agreement with the experimental results is very good, with the vapor and liquid densities and vapor pressures only very slightly too high. The previous work on atomic systems[2] suggests that the shift in both the saturated liquid and vapor densities could be an indication that the "crossing point" of the potential may be slightly in error and that additional interaction energy calculations at COM separation distances between 3.4 and 3.9 Å might improve the predictions. Also, a larger basis set might result in slightly more attractive interaction energies leading to lower predicted vapor pressures, though we did not pursue either hypothesis. However, it is important to note that the procedure we have proposed here has led to an accurate prediction of the experimental phase behavior without fitting to any experimental data other than the quadrupole moment.

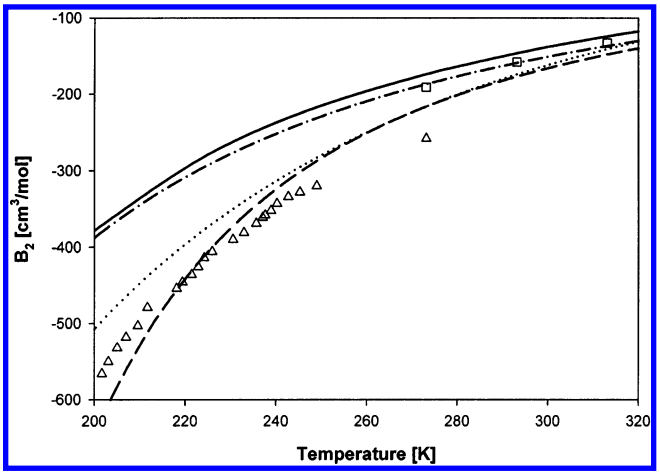

Figure 6. Second virial coefficients of acetylene. The triangles are the experimental data of Schafer;[37] the squares are the data of Bottomley et al.;[38,39] the dashed line is the correlation of Orbey[41] with the fourth parameter equal to −0.03; the dash-dot line is the correlation of Orbey with the fourth parameter equal to zero; the dotted line is the DIPPR correlation;[42] and the solid line is the result calculated using the final HM-IE MP2/3:CC potential.

The inclusion of three-body or multi-body effects may either improve or degrade the agreement with the experimental results depending on whether the effects increase the attractive molecular interactions, as is the case in hydrogen-bonding fluids such as methanol,[32] or decrease the attractive molecular interactions, as is the case for rare gases.[33−35] Using the isotropic, triple-dipole coefficient for acetylene[36] to estimate the three-body energy for three acetylene molecules 4.2 Å apart (the first maximum of the COM radial distribution function), we obtain a value of 0.18 kJ/mol, which, when split between the three distinct pairs of molecules, is likely with the accuracy of the quantum chemical calculations and the potential fit. Therefore, we expect the effect of nonpairwise additivity to be relatively small and indistinguishable within our work, such that it seems reasonable to neglect multi-body contributions at this time.

The new potential can be used to resolve a discrepancy between sets of reported experimental second virial coefficients[37−39] as well. Figure 6 shows the good agreement between the second virial coefficients calculated using the final potential and the experimental data of Bottomley et al.[38,39] However, there is significant disagreement with the measured values of Schafer[37] over the entire temperature range, from 200 to 275 K. Given the good agreement with the results of Bottomley et al.[38,39] for 270 K and above, and the agreement with the experimental vapor−liquid-phase behavior from 200 to 290 K, it is likely that the experimental results of Schafer[37] are erroneous, though Schafer reported an estimated error of only 2% in his results.

The data of Schafer and of Bottomley et al. are the only two sets of data for acetylene that appear in an extensive compilation of second virial coefficients.[40] This compilation was used by Orbey[41] for his second virial coefficient correlation in which he included a nonzero fourth parameter for acetylene, thus treating acetylene as a "nonstandard" fluid.[41] The results in Figure 6 indicate that acetylene should not be treated as a "nonstandard" fluid and that this fourth parameter for acetylene in Orbey's correlation should instead be set to zero. The work of Schafer is also listed as a "primary accepted reference" within the DIPPR database[42] and used to determine the DIPPR correlation for the second virial coefficient of acetylene. The correlation reported there appears to be a compromise between

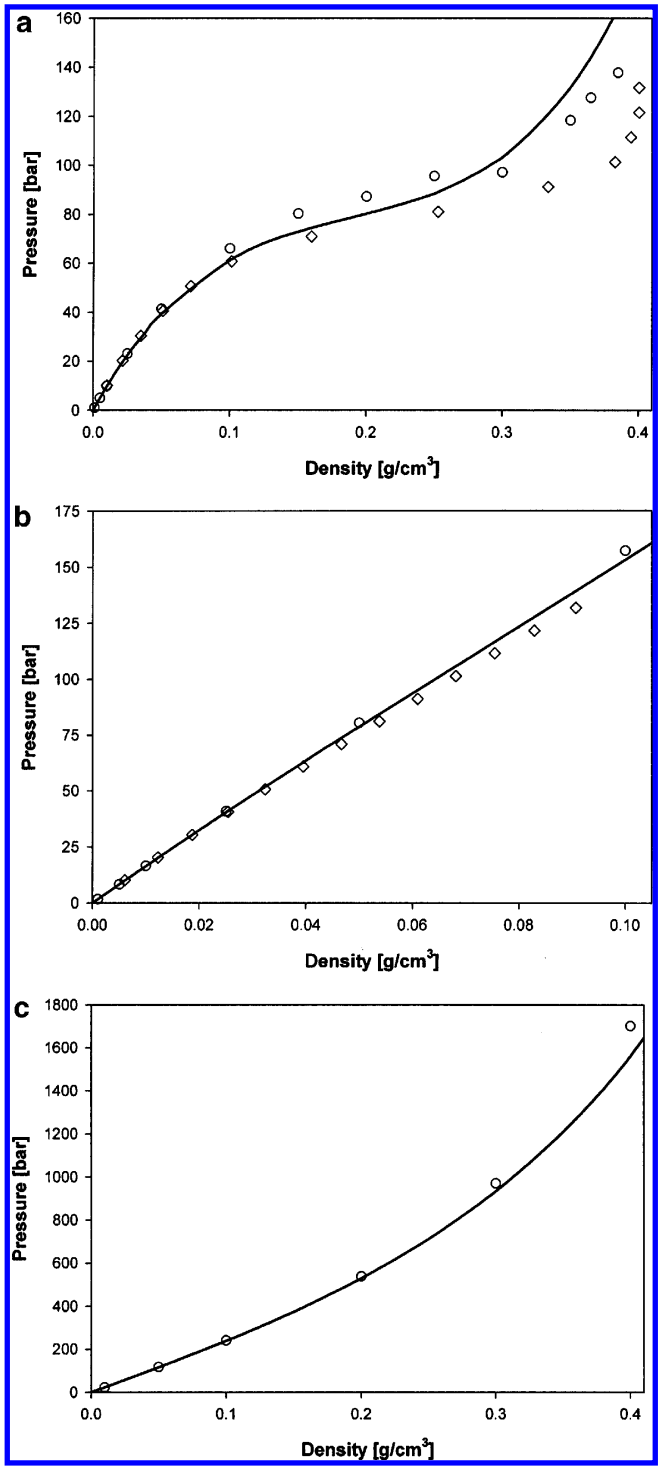

Figure 7. *PVT* curves for acetylene: (a) 323.15, (b) 523.15, and (c) 723.15 K. The line is the generalized Peng−Robinson equation of state, the circles are the results with the final HM-IE MP2/3:CC potential, and the diamonds are the experimental results.[43]

what we believe to be the more accurate results of Bottomley et al. and the inaccurate results of Schafer, and therefore should be reevaluated. These results demonstrate how molecular simulation and ab initio potentials obtained from quantum mechanics can be useful complements to experiment.

We also performed several *NVT* ensemble Monte Carlo simulations at supercritical conditions using the final intermolecular potential with 20 000 cycles for equilibration and at least 40 000 cycles for each production run. Again, standard long-range corrections were applied, and the choice of molecule for each translation and rotation was random to ensure microscopic reversibility. Simulations were run at 323.15, 523.15, and 723.15 K and compared with experimental data available at 323.15 and 523.15 K.[43]

Figure 7 shows the good agreement with the experimental results for all conditions. Excellent agreement is obtained for pressures below about 50 bar. Although the generalized Peng−Robinson equation of state better matches the pressures for intermediate densities at 323.15 K, the simulation results are more accurate at densities above 0.3 g/cm^3 and pressures above 100 bar. At 723 K, the Boltzmann factor an energy of +2 kJ/mol is 0.72 indicating that the high-energy configurations ignored in the final fit could be of some importance at these higher temperatures. However, given that the simulations contain no adjustable parameters and were not fit to any *PVT* data, these results again show the usefulness of property predictions from molecular simulations and ab initio potentials, especially at high-temperature, high-pressure, or other hazardous conditions. Additionally, these results show that ab initio potentials from quantum chemistry are applicable to conditions beyond those for which they were initially "designed."

Conclusion

The results of this work show that, in a reasonable amount of computer time (especially with a cluster of PCs), quantum chemical methods can give sufficiently accurate interaction energies to obtain intermolecular potentials that lead to predictions of thermodynamic properties such as saturation densities and pressures, second virial coefficients, and *PVT* behavior of good to excellent accuracy. We have also developed a reasonable prescription for obtaining an intermolecular potential for the calculation of accurate properties from molecular simulations for cases where pairwise additivity is a reasonable assumption. This procedure entails (1) calculating accurate quantum chemical interaction energies for a large number of random orientations for pairs of molecules at center-of-mass separation distances near those of the minimum energy configuration, (2) fitting a preliminary potential to these interaction energies, (3) using this potential in molecular simulations to obtain center-of-mass radial distribution functions and angular distributions at the conditions of interest, (4) using these results to identify the center-of-mass separation distances, orientations, and energies that are most important in the dense phase, (5) calculating additional energies for these important orientations and for all orientations at additional center-of-mass separation distances to better cover the long-range region, the "well region," and the "crossing point" of the molecular system as described by the center-of-mass pair distribution function, and (6) using Boltzmann-style weighting when fitting the intermolecular potential to weight the most important energies and configurations at the conditions of interest.

The interaction potential for acetylene obtained in this manner resulted in excellent vapor−liquid-phase behavior predictions, good second virial coefficient predictions that also resolved a discrepancy between reported experimental results, and good *PVT* predictions. Additionally, thermodynamic property predictions were obtained at conditions that are not easily or safely amenable to experiment. The procedure developed for obtaining an accurate intermolecular potential is likely applicable to other small and medium size molecular systems when pairwise additivity is a reasonable assumption, and the method developed can be especially useful for systems and/or conditions that are difficult or dangerous experimentally.

Acknowledgment. Financial support for this research was provided by the National Science Foundation (CTS-0083709) and the Department of Energy (DE-FG02-85ER13436). S.L.G. thanks Jeffery B. Klauda for helpful discussions concerning the fitting of the intermolecular potentials and Professor Norman J. Wagner and Armin W. Opitz for translation of portions of Schafer's paper.[37]

References and Notes

(1) Klauda, J. B.; Garrison, S. L.; Jiang, J. W.; Arora, G.; Sandler, S. I. *J. Phys. Chem. A* **2004**, *108*, 107.
(2) Garrison, S. L.; Sandler, S. I. *J. Chem. Phys.* **2002**, *117*, 10571.
(3) Tao, F. M.; Pan, Y. K. *J. Chem. Phys.* **1992**, *97*, 4989.
(4) Burcl, R.; Chalasinski, G.; Bukowski, R.; Szczesniak, M. M. *J. Chem. Phys.* **1995**, *103*, 1498.
(5) Williams, H. L.; Mas, E. M.; Szalewicz, K.; Jeziorski, B. *J. Chem. Phys.* **1995**, *103*, 7374.
(6) Koch, H.; Fernandez, B.; Christiansen, O. *J. Chem. Phys.* **1998**, *108*, 2784.
(7) Cybulski, S. M.; Toczylowski, R. R. *J. Chem. Phys.* **1999**, *111*, 10520.
(8) van de Bovenkamp, J.; van Duijneveldt, F. B. *Chem. Phys. Lett.* **1999**, *309*, 287.
(9) Curtiss, L. A.; Raghavachari, K.; Redfern, P. C.; Rassolov, V.; Pople, J. A. *J. Chem. Phys.* **1998**, *109*, 7764.
(10) Curtiss, L. A.; Redfern, P. C.; Raghavachari, K.; Rassolov, V.; Pople, J. A. *J. Chem. Phys.* **1999**, *110*, 4703.
(11) Dunning, T. H.; Peterson, K. A. *J. Chem. Phys.* **2000**, *113*, 7799.
(12) Frisch, M. J.; Trucks, G. W.; Schlegel, H. B.; Scuseria, G. E.; Robb, M. A.; Cheeseman, J. R.; Zakrzewski, V. G.; Montgomery, J. A.; Stratmann, R. E.; Burant, J. C.; Dapprich, S.; Millam, J. M.; Daniels, A. D.; Kudin, K. N.; Strain, M. C.; Farkas, O.; Tomasi, J.; Barone, V.; Cossi, M.; Cammi, R.; Mennucci, B.; Pomelli, C.; Adamo, C.; Clifford, S.; Ochterski, J.; Petersson, G. A.; Ayala, P. Y.; Cui, Q.; Morokuma, K.; Malick, D. K.; Rabuck, A. D.; Raghavachari, K.; Foresman, J. B.; Cioslowski, J.; Ortiz, J. V.; Stefanov, B. B.; Liu, G.; Liashenko, A.; Piskorz, P.; Komaromi, I.; Gomperts, R.; Martin, R. L.; Fox, D. J.; Keith, T.; Al-Laham, M. A.; Peng, C. Y.; Nanayakkara, A.; Gonzalez, C.; Challacombe, M.; Gill, P. M. W.; Johnson, B. G.; Chen, W.; Wong, M. W.; Andres, J. L.; Head-Gordon, M.; Replogle, E. S.; Pople, J. *Gaussian 98*, Revision A.9; Gaussian, Inc.: Pittsburgh, PA, 1998.
(13) Boys, S. F.; Bernardi, F. *Mol. Phys.* **1970**, *19*, 553.
(14) van Duijneveldt, F. B.; van Duijneveldt-van de Rijdt, J. G. C. M.; van Lenthe, J. H. *Chem. Rev.* **1994**, *94*, 1873.
(15) Liu, B.; McLean, A. D. *J. Chem. Phys.* **1973**, *59*, 4557.
(16) Fuller, N. G.; Rowley, R. L. *Int. J. Thermophys.* **2000**, *21*, 45.
(17) Powles, J. G.; Davis, C.; Evans, W. A. B.; Murad, S. *Mol. Phys.* **1990**, *70*, 529.
(18) Pawlowski, F.; Jorgensen, P.; Olsen, J.; Hegelund, F.; Helgaker, T.; Gauss, J.; Bak, K. L.; Stanton, J. F. *J. Chem. Phys.* **2002**, *116*, 6482.
(19) Karpfen, A. *J. Phys. Chem. A* **1999**, *103*, 11431.
(20) Wormer, P. E. S.; Hettema, H. *J. Chem. Phys.* **1992**, *97*, 5592.
(21) Wormer, P. E. S.; Hettema, H. *POLCOR package*; University of Nijmegen: The Netherlands, 1992.
(22) Rowley, R. L.; Pakkanen, T. *J. Chem. Phys.* **1999**, *110*, 3368.
(23) Rowley, R. L.; Yang, Y.; Pakkanen, T. A. *J. Chem. Phys.* **2001**, *114*, 6058.
(24) Delhommelle, J.; Millie, P. *Mol. Phys.* **2001**, *99*, 619.
(25) Allen, M. P.; Tildesley, D. J. *Computer Simulations of Liquid*; Oxford Press: Oxford, UK, 1987.
(26) Frenkel, D.; Smit, B. *Understanding Molecular Simulation*: *From Algorithms to Applications*; Academic Press: New York, 1996.
(27) Ambrose, D. *Ttans. Faraday Soc.* **1956**, *52*, 772.
(28) Ambrose, D.; Townsend, R. *Trans. Faraday Soc.* **1964**, *60*, 1025.
(29) Tsonopoulos, C.; Ambrose, D. *J. Chem. Eng. Data* **1996**, *41*, 645.
(30) *Perry's Chemical Engineers' Handbook*, 7th ed.; Perry, R. H., Green, D. W., Maloney, J. O., Eds.; McGraw-Hill: New York, 1997.
(31) Sum, A. K.; Sandler, S. I. *Mol. Phys.* **2002**, *100*, 2433.
(32) Sum, A. K.; Sandler, S. I.; Bukowski, R.; Szalewicz, K. *J. Chem. Phys.* **2002**, *116*, 7627.
(33) Leonhard, K.; Deiters, U. K. *Mol. Phys.* **2000**, *98*, 1603.
(34) Nasrabad, A. E.; Deiters, U. K. *J. Chem. Phys.* **2003**, *119*, 947.
(35) Bukowski, R.; Szalewicz, K. *J. Chem. Phys.* **2001**, *114*, 9518.
(36) Kumar, A.; Meath, W. J. *Mol. Phys.* **1992**, *75*, 311.
(37) Schafer, K. *Z. Phys. Chem. Abt. B* **1937**, *B36*, 85.
(38) Bottomley, G. A.; Reeves, C. G.; Seiflow, G. H. F. *Nature* **1958**, *182*, 596.
(39) Bottomley, G. A.; Reeves, C. G.; Seiflow, G. H. F. *J. Appl. Chem.* **1959**, *9*, 517.
(40) Dymond, J. H.; Smith, E. B. *The Virial Coefficients of Pure Gases and Mixtures*: *A Critical Compilation*; Oxford University Press: New York, 1980.
(41) Orbey, H. *Chem. Eng. Commun.* **1988**, *65*, 1.
(42) Rowley, R. L.; Wilding, W. V.; Oscarson, J. L.; Zundel, N. A.; Marshall, T. L.; Daubert, T. E.; Danner, R. P. *DIPPR Data Compilation of Pure Compound Properties*; AIChE: New York, 2001.
(43) Teranishi, H. *Rev. Phys. Chem. Jpn.* **1955**, *25*, 25.